Check for updates

The role of tidal creeks in shaping carbon and nitrogen patterns in a Chinese salt marsh

Ziwen Ma, Yanan Wu, Siqi Zhao, Yueyan Pan, Jiakai Liu, Mingxiang Zhang* and Zhenming Zhang*

College of Ecology and Nature Conservation, Beijing Forestry University, Beijing, China

Tidal creeks play a crucial role in lateral transport of carbon and nutrients from tidal salt marshes. However, the specific impact of tidal creek development on carbon and nutrient distribution within the marsh remains poorly understood. The objective of this study is to assess the influence of lateral tidal flooding through the tidal creeks on the spatial distribution of carbon and nitrogen fractions in the soils of a Chinese temperate salt marsh. We conducted a comprehensive analysis of the relative variations in different carbon and nitrogen fractions, along with soil physicochemical and microbial indicators, between the bank soil of the tidal creek and its lateral inland soils across high, middle, and low flats. Our findings highlight that tidal creek development significantly affects the middle flat, leading to substantial variations in organic carbon and total nitrogen. The low flat mainly experiences changes in dissolved inorganic carbon levels. Furthermore, a lateral increase in microbial biomass is observed in the middle flat, indicating that the significantly lower SOC in the middle flat might be ascribed to enhanced microbial decomposition. The lateral enrichment of dissolved inorganic carbon in the low flat is possibly related to the nearshore location and/or abiotic adsorption in inorganic carbon sequestration. Overall, this study demonstrates the critical role of tidal creek development in shaping the distribution patterns of carbon and nitrogen fractions in tidal salt marshes.

KEYWORDS

blue carbon, nitrogen, tidal creek, salt marsh, Yellow River Delta

1 Introduction

Tidal wetlands, occurring in geomorphic settings with constant exchange of water and matter (dissolved and particulate) with adjacent estuaries, play a critical role in hydrological and biogeochemical cycling at the land-sea interface on local to global scales (Mcleod et al., 2011; Duarte et al., 2013; Santos et al., 2019; Webb et al., 2019). Salt marshes, widely thriving in tidal wetlands, are regarded as blue carbon ecosystems together with mangroves and seagrass beds, and are the most efficient soil carbon sinks on Earth on an areal basis

(Mcleod et al., 2011; van Ardenne et al., 2018). With the increasing global recognition of the significant role of blue carbon ecosystems in sequestrating carbon and mitigating climate change (Atwood et al., 2017), numerous studies have been conducted to quantify soil carbon stocks and explore the specific processes of carbon cycling in these ecosystems (Sanders et al., 2016; Asanopoulos et al., 2021; Santos et al., 2021).

Tidal creeks, cutting through low permeable salt marsh mud, are crucial in the transportation of carbon and nutrients, where they can export these materials through the flushing of plant and sediment materials or import marine organic matter over a full tidal period (Krest et al., 2000; Odum, 2002; Call et al., 2019; Tan et al., 2020). The sediment found on the banks and the suspended matter in the water can originate from tidal-driven erosion or resuspension occurring in adjacent tidal creeks (Fagherazzi et al., 2013). Additionally, tidal creeks serve as a link between surface marsh soils and tidal creek waters, which eventually connect to the ocean and/or the atmosphere through porewater exchange (Santos et al., 2019). Furthermore, tidal creeks function in directly connecting surface waters with underlying aquifers, where submarine groundwater discharge has been recognized as a significant exchange mechanism between land and sea (Taniguchi et al., 2019; Glaser et al., 2021).

Areas within the coastal ocean carbon cycle that remain uncertain have been subjected to decades of research (Windham-Myers et al., 2018). The question of whether salt marshes act as sinks or sources to adjacent estuaries has long been debated. Previous studies have suggested that this may be influenced by factors such as vegetation type (e.g., Tan et al., 2020), and/or tidal extent and magnitude (e.g., Regier et al., 2021). Furthermore, different carbon pools demonstrate distinct variation patterns in tidal creek-mediated lateral carbon fluxes. For example, research conducted on Taskinas Creek, a temperate tidal marsh creek system in the York River Estuary, revealed that the salt marsh acted as a sink for particulate organic carbon (POC) and a source of dissolved inorganic carbon (DIC) (Knobloch et al., 2021). In contrast, dissolved organic carbon (DOC) levels showed little variation across tidal stages (Knobloch et al., 2021). In another study conducted on Chongming Dongtan wetland, a temperate tidal salt marsh in the Yangtze estuary, it was found that the Poaceae creek served as a source of DOC and DIC throughout the year and as a sink of POC and particulate inorganic carbon (PIC) seasonally (Tan et al., 2020). Additionally, the Cyperaceae creek acted as a source of all investigated carbon components consistently throughout the year (Tan et al., 2020).

Great efforts have been made to quantify lateral outwelling carbon fluxes through spatial and temporal investigations in creek waters. However, little is known about the impact of tidal creek development on the spatial distribution of carbon and nutrient within the marsh itself. This lack of information also means that the relationship between carbon sequestration and environmental or geomorphic characteristics has not been well established. The changing climate, with its shifts in tidal extent and coastal geomorphology due to sea level rise, increased storm activity, and altered precipitation patterns, will have a significant impact on the role of tidal marsh systems in the coastal carbon cycle (Gabler et al.,

2017; Ensign and Noe, 2018). Therefore, it is essential to have reliable estimates of the effect of tidal creek development on carbon and nutrient distribution and the potential drivers under current hydrological conditions. Such information would greatly enhance our understanding of the biogeochemical processes that influence carbon in the coastal zone (Knobloch et al., 2021).

Our previous investigations found that soil inorganic carbon (SIC) distribution was significantly influenced by sedimentary processes from land to sea, demonstrating a clear seaward decreasing trend (Ma et al., 2024). Conversely, soil organic carbon (SOC) did not exhibit consistent variation patterns from land to sea, which is thus hypothesized to be related to the development of tidal creeks in the tidal flat. This hypothesis is based on previous findings that biological activities, such as the growth of vegetation (Wu et al., 2021), seed fluxes and germination (Wu et al., 2023a, 2023b) in tidal flats can be influenced by tidal creek development. Additionally, substantial variations in tidal creek distribution patterns were observed among high, middle, and low flats, resulting in significant effects on soil moisture and salinity gradients (Wu et al., 2020). Therefore, we propose that the spatial distribution of different carbon and nitrogen fractions in tidal salt marshes would also respond differently to varying tidal creek development. However, SOC distribution could also be impacted by the sedimentary process from land to sea, so it was hard to further verify the role of tidal creeks in impacting carbon and nutrient distribution without excluding the influence of the original sedimentation in affecting SOC variation. Therefore, we investigated the relative variations of different carbon and nitrogen fractions between the bank soil and its perpendicularly flooding inland soils along the creek-perpendicular sampling transect at high, middle, and low flats. The bank soil of tidal creek underwent the highest hydrodynamical energy and constant scouring of seawater, which significantly limited biological activities, such as seed settling and plant growth (Bouma et al., 2009; Lai et al., 2018). As seawater floods into the marsh through the creek, the hydrodynamic forces weakened and gradually created suitable soil environments for salt-tolerated plants to thrive (Wang et al., 2021). The barren bank soil was accordingly regarded as the starting point of the impact of the development of tidal creeks for saltmarshes. The calculation of the relative variation of different carbon and nitrogen fractions between the bank soil and lateral inland soil in each creek-perpendicular transect can eliminate the originally vertical sedimentary effects on their distribution from land to sea. Comparison of the relative variations of different carbon and nitrogen fractions among high, middle and low flats were intended to demonstrate the potentially different role of lateral tidal flooding through the tidal creeks in shaping the distribution patterns of carbon and nitrogen in tidal salt marshes.

2 Materials and methods

2.1 Site description

The study was conducted in the Yellow River Delta (YRD), which is the youngest and largest coastal wetland in temperate

China with a high biodiversity level. This region is featured by a continental monsoon climate as the annual mean temperature of 12-13°C and average annual precipitation of 560-590 mm (Ning et al., 2023). The soil type along the coastline, identified as Calcaric Fluvisols and Gleyic Solonchaks, is mainly derived from the Loess Plateau in the middle and upper reaches of the Yellow River. The tides in this region are irregular and semi-diurnal, with the average tidal amplitude ranging from 1.1 to 1.5 m (Chang et al., 2022). The salt marsh plants were distributed in the intertidal zone. Among them, the *Suaeda salsa* is the dominant therophyte and pioneer species in the tidal native salt marsh of the YRD, distributing from middle to high marshes. The *S. salsa* tidal salt marsh is formed due to the development of numerous tidal creeks, which bring enough seeds and sustain suitable hydrologic and saline environments for the growth of *S. salsa* (Wang et al., 2021). In turn, the *S. salsa* tidal salt marshes provide pivotal stopover habitats for millions of migratory shorebirds of the East Asian-Australasian Flyway (Studds et al., 2017). These marshes, also known as the iconic "Red Beach," not only support a vast number of migratory shorebirds but also have substantial economic and tourism potential (Ren et al., 2021). To study the relationship between the spatial distribution of carbon and nitrogen fractions and the development of tidal creeks, the study area (119°9′~119°11′ E, 37°46′ ~37°49′ N) chosen was a region with a relatively complete and undisturbed tidal creek network (Figure 1).

2.2 Soil collection and analysis

Before the field sampling, the tidal creek in the high, middle, and low flat of the YRD was identified using aerial images. Two sample transects were then established in the high, middle, and low flats of the study area, respectively, following the direction of the vertical tidal creek. A total of six transects were set up from the seaward to the landward (Figure 1). In each sampling transect, five plots were designated at 0, 10, 20, 30, and 40 m. Due to the great hydrodynamical energy and constant scouring of seawater it underwent, the bank soil of tidal creek barely supported plant growth. Therefore, the bank soil at the 0 m plot served as the reference soil, while the soils at the rest plots of the same transect were considered inland soils. Soil samples were collected separately

from each plot, including a five-multi-point mixed surface soil sample (0-10 cm) and a cutting ring surface soil sample. Vegetation information of the high, middle, and low flat has been recorded based on both unmanned aerial vehicle (UAV) aerial photography and field surveys in another study (Wu et al., 2020). It is worth mentioning that the sampling focused on shallow soil depths (0-10 cm) to ensure the recent influence of the tidal marsh creek system was captured, rather than historical influences from greater depth within the soil profile (Kelleway et al., 2017; Asanopoulos et al., 2021). During the sampling process, all wetland soil samples were collected during low tide to eliminate any additional effects of tides. A total of 30 soil samples and 30 cutting ring samples were collected in March 2021, which marked the beginning of the growing season with the least precipitation throughout the year. This timing was chosen to minimize the impact of other hydrological processes on the distribution of carbon and nitrogen fractions driven by the local climate. Within a week, all collected soil samples were transported to the laboratory. Prior to analysis, visible roots and debris were manually removed, and each sample was divided into three parts. One part was utilized for physical and chemical analysis, another part was stored at 4°C for the measurement of microbial biomass within a week, and the third part was freeze-dried and preserved in a refrigerator at -80°C to determine the phospholipid fatty acids (PLFAs) content in the soils.

The bulk density (BD) and moisture were measured by drying cutting ring samples at 105°C for 24 h, and further salt correction was calculated for BD measurement (Lavelle et al., 1985). The soil pH was determined using a HANNA pH meter (Hanna Instruments, Woonsocket, RI, USA) with a soil to water ratio of 1:5. Electric conductivity (EC) was measured in the supernatant of 1:5 soil-water mixtures using an EC meter (VWR Scientific, West Chester, PA, USA). The soil texture was characterized by analyzing the soil particle size distribution with a laser particle size analyzer (SEDIMAT 4–12, Germany), after the removal of organic matter by digestion in a heated hydrogen peroxide solution with sodium hexametaphosphate as a dispersing agent (Peng et al., 2014). The total carbon (TC) and total nitrogen (TN) contents were quantified using an elemental analyzer (Heraeus Elementar Vario EL, Hanau, Germany). SOC was measured using the dichromate oxidation method (Anderson and Domsch, 1989), on dried and sieved soils with a particle size of 0.149 mm. SIC was calculated as the difference
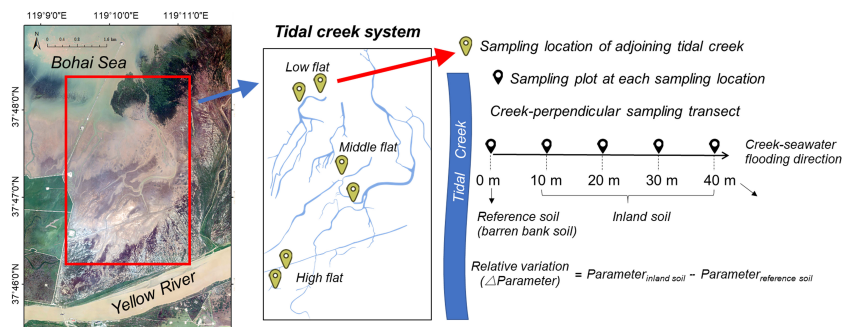

FIGURE 1
Location map of sampling sites in the Yellow River Delta, China.

between TC and SOC. The microbial biomass carbon (MBC) and microbial biomass nitrogen (MBN) were measured using the chloroform fumigation-extraction (CFE) method (Vance et al., 1987), as described by Ma et al. (2017). The DOC and DIC were measured using a total organic carbon analyzer (TOC-V, Shimadzu, Kyoto, Japan), with soil extracts obtained by shaking a mass ratio of soil to water of 1:10 for 24 h in the dark and passing through 0.45 μm filter membranes.

Soil PLFAs were identified based on a modified single-phase extraction according to Bossio et al. (1998), as described by Ma et al. (2017). Total PLFAs (TotPLFA), which were calculated as the sum of PLFAs with more than 1% of the total relative abundance, served as an overall indicator of microbial biomass. Bacterial PLFAs (BacPLFA) were calculated as the sum of 14:0, i15:0, a15:0, 15:0, i16:0, 16:1ω9c, 16:1ω7c, 16:0, 16:1ω7cDMA, i17:0, a17:0, 17:1ω8c, 17:1ω6c, cy17:0, 17:0, 18:1ω7c, 18:1ω5c, 18:0, cy19:0 (García-Orenes et al., 2013). Branched phospholipids i15:0, a15:0, i16:0, i17:0, a17:0 were used as gram-positive bacterial biomarkers (GpPLFA), and gram-negative bacterial biomass (GnPLFA) were assessed by 16:1ω9c, 16:1ω7c, 17:1ω8c, 17:1ω6c, cy17:0, 18:1ω7c, 18:1ω5c, cy19:0 (Olsson et al., 1995; García-Orenes et al., 2013). Fungal PLFAs (FungalPLFA) were quantified by summing 18:2ω6c and 18:1ω9c (Frostegård and Bååth, 1996; Olsson, 1999). Actinomycetes PLFAs (ActinoPLFA) were calculated as the sum of 10Me fatty acids (Zelles et al., 1995). The fatty acid 16:1ω5c was employed as an indicator of arbuscular mycorrhizal fungi (AMFungalPLFA) (Olsson et al., 1995), and the presence of protozoa was determined by the abundance of 20:4ω6c (ProtozoaPLFA) (Doran et al., 2007).

2.3 Statistical analysis

Soil carbon/nitrogen fraction stocks (g/m^2) in total soils were calculated as:

$$Soil carbon/nitrogen fraction stocks = D \times BD \times C \times 10$$

where D was the thickness (cm) of the soil layer, BD was the bulk density (g/cm^3) and C was the contents (g/kg) of corresponding carbon/nitrogen fraction (including TC, SOC, DOC, MBC, SIC, DIC, TN, MBN) at the 0-10 cm soil depth.

Relative variations of soil physicochemical properties/microbial PLFAs/carbon and nitrogen fraction concentrations and stocks were calculated as:

$$Relative variations of single parameter (\Delta Parameter)$$
$$= Parameter_{inland soil} - Parameter_{reference soil}$$

Data analysis and figure creation were carried out using R v.4.1.1 (R Development Core Team, 2021). Prior to statistical analysis, tests for normality on the raw data were performed. One-way analyses of variance with a Tukey's honestly significant difference *post hoc* test were used to assess differences among high, middle and low flats (P< 0.05). Principle component analysis (PCA) was conducted to identify the spatial differences of sampling sites and explore potential relationship among relative variations of soil

physicochemical properties, microbial parameters and carbon and nitrogen fraction concentrations and stocks.

3 Results

Two simplified effects, including vertical sedimentation effect and lateral tidal effect through the development of tidal creeks, on the distribution patterns of carbon and nitrogen fractions were illustrated in Figure 2. Accordingly, the absolute values of soil metrics in different locations relative to the seashore primarily reflected the effect of sedimentary processes on the soil from land to sea. While the relative variations calculated in this study were aimed to eliminate the vertical sedimentation effect and demonstrate the lateral tidal effect on the soil metrics.

3.1 Lateral tidal effect on soil physicochemical properties

The comparison of absolute values of soil physicochemical properties across high, middle and low flats showed relatively obvious vertical sedimentary characteristics from land to sea as indicated by soil texture, BD, moisture and EC (Supplementary Figure S1). Specifically, soil texture tended to be coarser and BD tended to be greater in the seaward side of tidal flats. This is largely due to the vertical influence of tidal seawater on the transportation and deposition of soil particles, as finer soils were more easily transported by water flow compared to coarser ones (Nguyen et al., 2013). These vertical sedimentary characteristics played a dominant role in creating a water-salt gradient from land to sea, as well (Rabot et al., 2018). When eliminating the vertical sedimentary effect by calculating the relative variation of inland soils relative to the reference soil, it could be observed that the locations of tidal flats relative to the seashore also exert distinct effects on soil texture and salinity in relation to the development of tidal creeks. In the middle
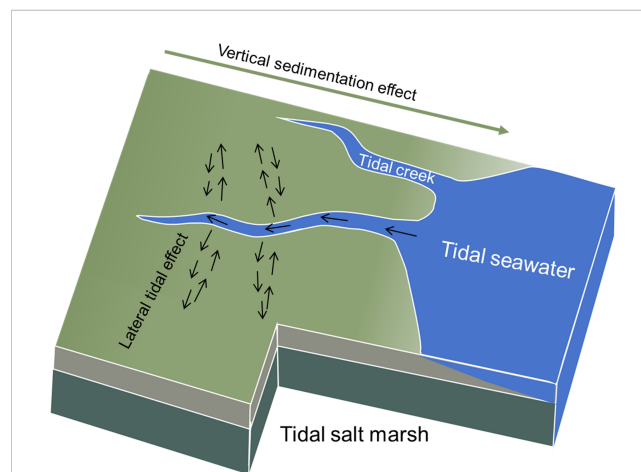

FIGURE 2
A simplified conceptual diagram of the role of tidal creeks in exerting lateral effect on the distribution patterns of carbon and nitrogen fractions in salt marsh.

flat, the lateral inland soils showed lower clay contents compared to the reference soil, and their relative variations were all below 0 (Figure 3E). However, the relative variations of clay content in high and low flats were roughly all above 0, and significantly higher than those in the middle flat (Figure 3E). Conversely, the middle flat exhibited significantly higher relative variations of sand content compared to high and low flats (Figure 3G). This suggests that the lateral deposition of large-sized soil particles in tides through the development of tidal creeks tends to occur more in the middle flat than in high and low flats. Moreover, the high flat exhibited significantly higher relative variations of soil EC compared to the middle and low flats (Figure 3D). This indicates that the development of tidal creeks in the high flat leads to the accumulation of soil salinity in their lateral flooding inland soils. However, no statistically significant difference was found in the relative variations of soil moisture, pH, and silt content across high, middle, and low flats.

3.2 Lateral tidal effect on soil PLFAs

Both the vertical sedimentation processes and lateral tidal flooding exert similar effects on the distribution of soil PLFAs indicative of most taxonomic soil microbes, as significantly higher absolute contents and relative variations of TotPLFA, BacPLFA, GpPLFA, GnPLFA, FungalPLFA, ActinoPLFA, and AMFungalPLFA were

detected in the middle flat compared to high and low flats (Supplementary Figures S2, 4), indicating a enrichment of biomass of most microbial communities induced by both vertical sedimentation and lateral tidal effect. However, ProtozoaPLFA showed relatively different varied patterns from other PLFAs, as its absolute content was increased from land to sea, while there was no significant difference in the relative variation of ProtozoaPLFA across high, middle and low flats. This suggests that protozoa is likely to be affected by vertical sedimentary processes instead of lateral tidal flooding through the tidal creeks.

3.3 Lateral tidal effect on soil carbon and nitrogen contents and stocks

There was an increasing trend for SOC contents and stocks and decreasing trend for SIC contents and stocks along the vertical sedimentation gradient from land to sea, leading to overall insignificant changes in TC levels (Supplementary Figures S3–S5). However, there was no significant change in MBC, DOC, DIC, TN and MBN contents and stocks regarding the vertical sedimentation effect (Supplementary Figures S3–S5). Comparatively, when eliminating vertical sedimentation effect by calculating relative variations to the reference soil, it was shown that the development of tidal creeks showed a similar lateral impact on the contents and stocks of TC and SOC. The middle flat had
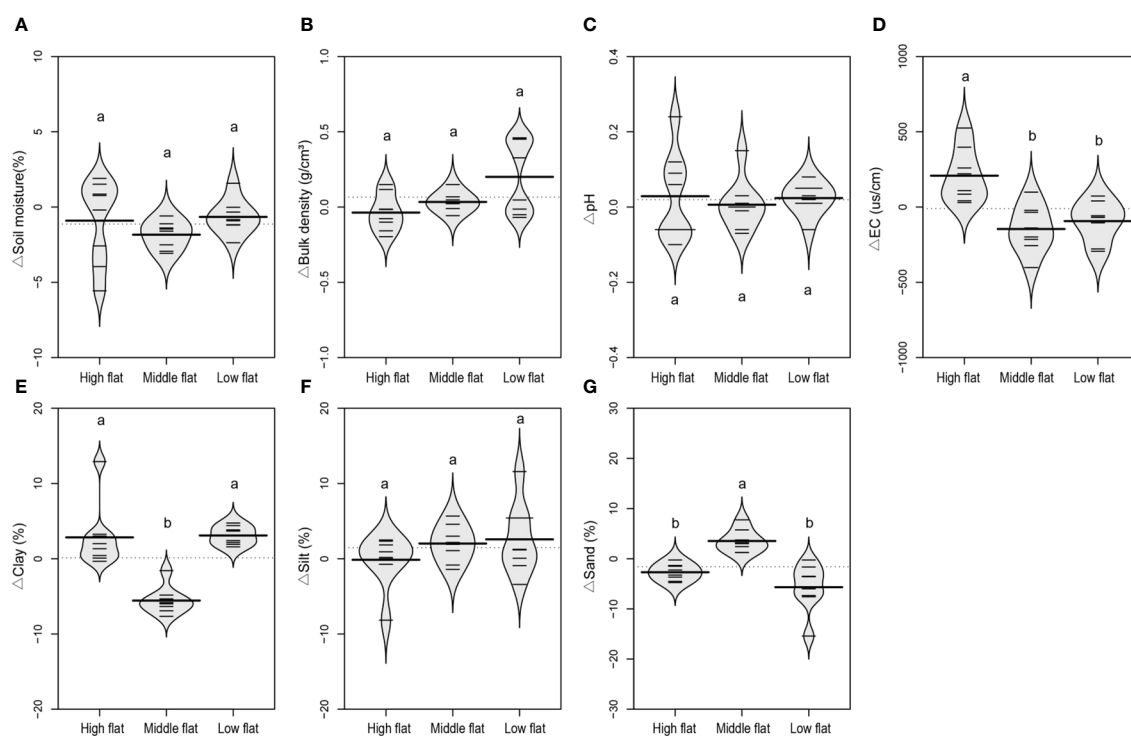

FIGURE 3
A beanplot of relative variation of inland surface (0-10 cm) soils (sampled at 10, 20, 30 and 40 m vertical distance from the tidal channel) to the reference soil (sampled at 0 m vertical distance from the tidal channel) in soil moisture **(A)**, bulk density **(B)**, pH **(C)**, electrical conductivity **(D)**, clay content **(E)**, silt content **(F)**, and sand content **(G)**. Individual observations are shown as small black lines and the median value with a longer black line. The grey area shows the distribution of concentrations (N = 8). Different lowercase letters (a, b) in the same graph indicate significant differences (P< 0.05).
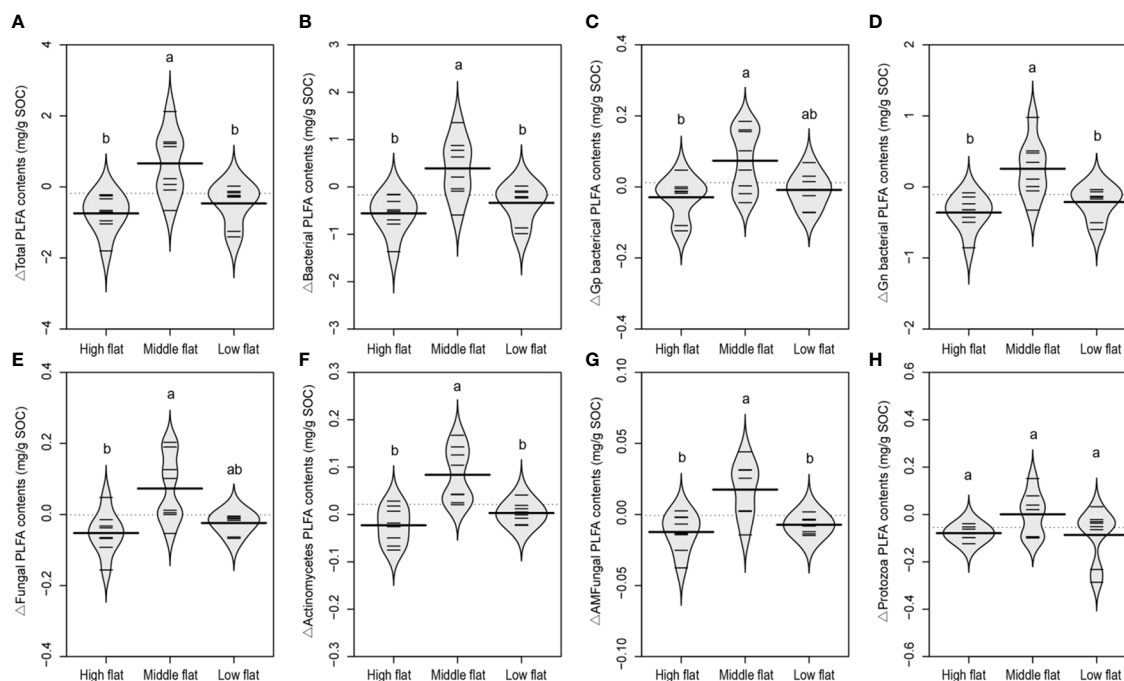
FIGURE 4
A beanplot of relative variation of inland surface (0-10 cm) soils (sampled at 10, 20, 30 and 40 m vertical distance from the tidal channel) to the reference soil (sampled at 0 m vertical distance from the tidal channel) in contents of total PLFA **(A)**, bacterial PLFA **(B)**, gram-positive bacterial PLFA **(C)**, gram-negative bacterial PLFA **(D)**, fungal PLFA **(E)**, actinomycete PLFA **(F)**, arbuscular mycorrhizal fungal PLFA **(G)**, and protozoa PLFA **(H)**. Individual observations are shown as small black lines and the median value with a longer black line. The grey area shows the distribution of concentrations (N = 8). Different lowercase letters (a, b) in the same graph indicate significant differences (P< 0.05).

significantly lower relative variations of TC and SOC compared to the high and low flats (Figures 5A, B, 6A, B). The same spatially divergent response to tidal creek development was observed for TN and MBN contents and stocks, with significantly lower relative variations in the middle flat than in the high and low flats (Figures 5E, F, 6E, F). This suggests that the middle flat accumulated less organic carbon and nitrogen induced by the lateral tidal effect within the zone. However, this divergence was not observed for DOC, MBC and SIC, as their relative variations of contents and stocks did not differ significantly among different flats (Figures 5–7). Interestingly, levels of DIC tended to be higher near the seashore with the effect of lateral tidal flooding, as relative variations of DIC contents and stocks were significantly higher in the low flat compared to the high and middle flats (Figure 7).

3.4 PCA of soil carbon and nitrogen fractions and soil physicochemical and microbiological properties

The spatial divergence in soil physicochemical, microbiological, and carbon and nitrogen parameters across the three tidal flats was illustrated using multivariate PCA (Figure 8). The PCA analysis revealed that PC1 and PC2 accounted for 44.12% and 16.70% of the variability in carbon and nitrogen contents, respectively (Figure 8A), and 44.35% and 12.41% of the variability in carbon and nitrogen stocks, respectively (Figure 8B). The location of the

sampling tidal flats relative to the seashore had a significant impact on the variability. Specifically, the PCA loading scores showed that the middle flat exhibited a distinct cluster along PC1, separate from the high and low flats, primarily due to significantly higher soil microbial PLFAs and lower SOC and clay content.

4 Discussion

4.1 The middle flat was a potential hotspot of carbon and nitrogen variation induced by lateral tidal effect

Based on the results of our investigations, the middle flat in tidal *S. salsa* salt marsh of the YRD exhibited significantly lower organic carbon and nitrogen levels under the influence of lateral tidal flooding compared to the high and low flats. Given the bank soil barely supported plant growth, the direct measurements of vegetation parameters could be equal to the relative variation calculated in this study. Therefore, variations of SOC and TN induced by lateral tidal effect tended to contradict that of vegetation, as previous studies showed that the middle flat had a denser growth of *S. salsa* and greater seed germination rates (Wu et al., 2021; Wu et al., 2023a, b). Typically, aboveground vegetation should have a positive influence on the accumulation of SOC through the input of plant detritus, root exudates, and particle trapping (Santini et al., 2019; Santos et al., 2019). However, in this
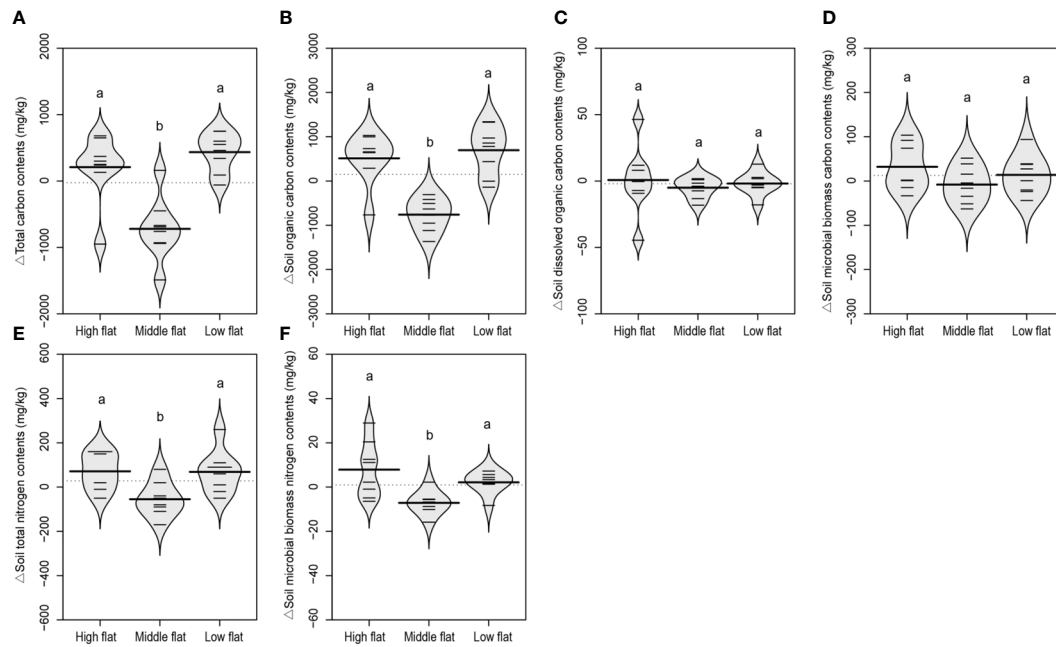
FIGURE 5
A beanplot of relative variation of inland surface (0-10 cm) soils (sampled at 5, 10, 20, 30 and 40 m vertical distance from the tidal channel) to the reference soil (sampled at 0 m vertical distance from the tidal channel) in soil total carbon contents **(A)**, organic carbon contents **(B)**, dissolved organic carbon contents **(C)**, microbial biomass carbon contents **(D)**, total nitrogen contents **(E)**, and microbial biomass nitrogen contents **(F)**. Individual observations are shown as small black lines and the median value with a longer black line. The grey area shows the distribution of concentrations (N = 8). Different lowercase letters (a, b) in the same graph indicate significant differences (P< 0.05).

FIGURE 6
A beanplot of relative variation of inland surface (0-10 cm) soils (sampled at 10, 20, 30 and 40 m vertical distance from the tidal channel) to the reference soil (sampled at 0 m vertical distance from the tidal channel) in soil total carbon stocks **(A)**, organic carbon stocks **(B)**, dissolved organic carbon stocks **(C)**, microbial biomass carbon stocks **(D)**, total nitrogen stocks **(E)**, and microbial biomass nitrogen stocks **(F)**. Individual observations are shown as small black lines and the median value with a longer black line. The grey area shows the distribution of concentrations (N = 8). Different lowercase letters (a, b) in the same graph indicate significant differences (P< 0.05).
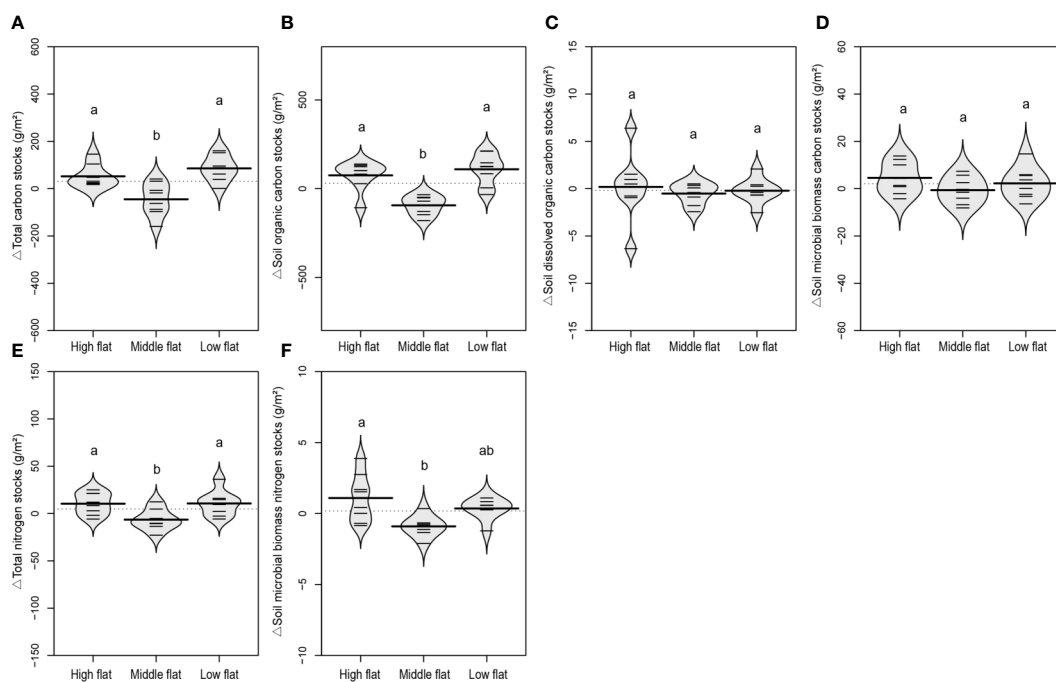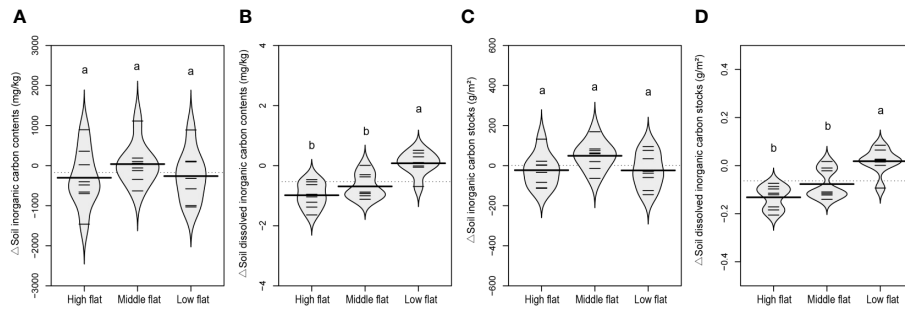
FIGURE 7
A beanplot of relative variation of inland surface (0-10 cm) soils (sampled at 10, 20, 30 and 40 m vertical distance from the tidal channel) to the reference soil (sampled at 0 m vertical distance from the tidal channel) in soil inorganic carbon contents **(A)**, dissolved inorganic carbon contents **(B)**, inorganic carbon stocks **(C)**, and dissolved inorganic carbon stocks **(D)**. Individual observations are shown as small black lines and the median value with a longer black line. The grey area shows the distribution of concentrations (N = 8). Different lowercase letters (a, b) in the same graph indicate significant differences (P< 0.05).

study, no such positive association was observed. Several potential explanations for this inverse pattern can be considered. Firstly, the higher germination rates and better connectivity of plant patches in the middle flat indicated potentially higher nutrient uptake, resulting in a significant reduction of SOC and TN concentrations and stocks. Secondly, the middle flat had a denser distribution of tidal creeks. Our previous investigations have found that the average branching rate and density of tidal creeks in the middle flat was 6.23 pcs/km^2 (pieces of bifurcation point per unit area) and 2.22 km/km^2 (lengths of tidal creeks per unit area), respectively, higher than the high flat (3.79 pcs/km^2, 1.44 km/km^2) and low flat (2.61 pcs/km^2, 2.21 km/km^2) (Wu et al., 2020). These morphological differences of tidal creeks potentially led to intensified hydrodynamic energy resulting from superimposed effect of multiple tidal creeks in the middle flat that weakened the trapping and sedimentation abilities of this area, thereby reducing the burial of SOC. This distinct pattern of sedimentation was further reflected in the composition of soil texture, with the middle flat exhibiting significantly more sand and less clay

content compared to the high and low flats (Figure 3). This reduction in clay content induced by lateral tidal effect could also contribute to the decreased SOC levels in the middle flat, as larger-sized soil particles bind less SOC due to their smaller surface areas (Pedersen et al., 2011).

Furthermore, higher relative variations of microbial biomass as indicated by soil PLFAs (Figure 4) and lower SOC levels were concomitant in the middle flat, suggesting enhanced microbial decomposition that could contribute to the decrease in sequestered SOC impacted by the lateral tidal flooding. Both the vertical and lateral enrichment of microbial biomass in the middle flat partly aligns with the intermediate disturbance hypothesis, which postulates that disturbances of an intermediate frequency or intensity maximize community biodiversity/richness (Odum, 1963). The distribution pattern and germination rates of *S. salsa* in tidal flats of the YRD have been previously demonstrated to respond in a curvilinear mode with the hydrologic connectivity (Wang et al., 2021; Wu et al., 2021). Coastal areas with intermediate disturbances have been reported to support more biodiversity albeit
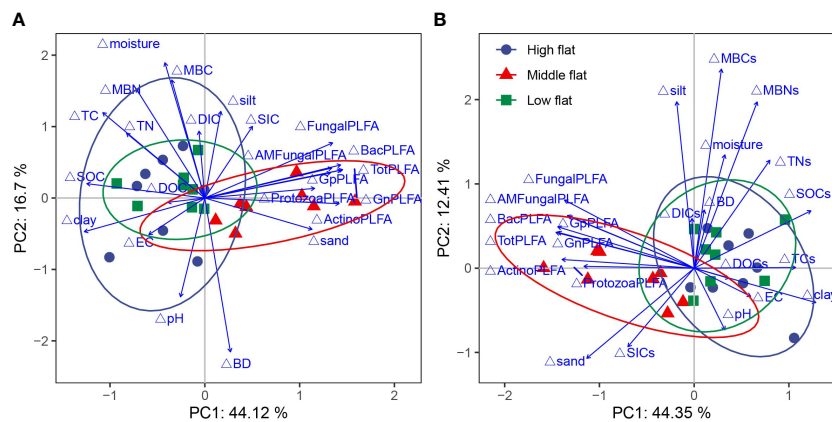
FIGURE 8
Principal component analysis (PCA) of relative variation of soil physicochemical properties, microbial parameters and carbon contents **(A)** and stocks **(B)** in tidal *S. salsa* saltmarsh in the YRD. Blue solid circles represent soils sampled in high flat, red solid triangles represent soils sampled in middle flat, and green solid squares represent soils sampled in low flat. Solid arrows are soil physicochemical properties and microbial parameters.

with disputes (England et al., 2008; Gerwing et al., 2017). This trend was partially followed by soil microbes, suggesting a potential interconnected network linking all biodiversity, from flora and fauna to soil microbes, which leads them to respond similarly to external disturbances. However, the regulating mechanisms of the enrichment of soil microorganisms in the middle flat and their connections to the ecological functions of salt marshes, such as carbon sequestration, require further verification and exploration.

4.2 Different carbon and nitrogen fractions exhibited varied responding patterns to the lateral tidal effect

In this study, there were no consistent patterns observed for the investigated carbon and nitrogen fractions in response to the lateral tidal effect. Specifically, although lateral tidal flooding through tidal creeks in the middle flat tended to reduce SOC, no significant difference was found for SIC levels. The relatively contrasting distribution pattern between SIC and SOC along the vertical sedimentation gradient from land to sea showed a negative interaction between SOC and SIC variations, which partly resulted from the limited packing density of the sedimentation process of organic matter fraction and mineral fraction of the soil (Breithaupt et al., 2017; Asanopoulos et al., 2021). However, no such contrasting variation pattern between SOC and SIC induced by the lateral tidal flooding through the tidal creeks was indicative of their distinct responding patterns to the development of tidal creeks. Furthermore, the insignificant difference in SIC variation may also be ascribed to its more complicated formation and transformation mechanisms that counteract with each other (Lal, 2008; Han et al., 2018). On the whole, our previous study conducted in the YRD has shown that SIC contents and stocks significantly decreased from land to sea, while SOC exhibited inconsistently varied pattern along the vertical sedimentation gradient (Ma et al., 2024). Taking the findings of this study and the previous study into consideration, it appears that SOC is likely to be more impacted by the lateral tidal flooding through the tidal creeks, whereas SIC is more influenced by the vertical sedimentary processes from land to sea.

Likewise, neither lateral tidal flooding nor vertical sedimentary processes exerted significant effects on DOC variation in tidal *S. salsa* salt marshes of the YRD. Previous studies exploring the contributions of marsh creek systems to the lateral export of carbon components reported that DOC did not show an obvious gradient across tidal stages, possibly due to the high processing of DOC within tidal creeks, which homogenized the signals from the estuary and marsh system (Santos et al., 2019; Knobloch et al., 2021). Accordingly, the homogenizing effect of tidal seawater entering the salt marsh with high residence time may also occur in soils, resulting in insignificant changes of DOC levels in tidal salt marshes. Additionally, despite the insignificant changes in DOC contents and stocks, the sources of DOC can be distinct, which can be indicated by CDOM and/or other analysis methods (Knobloch et al., 2021). Consequently, it is essential to incorporate other indicators of DOC dynamics in further studies to provide more information on its variation.

DIC exhibited a distinct distribution pattern with lateral enrichment in the low flat (Figure 7), which was different from other carbon and nitrogen fractions in this study. As an important component of outwelling carbon, DIC plays a crucial role in coastal carbon cycling, as its outwelling and subsequent oceanic storage is a potential mechanism for long-term carbon sequestration (Santos et al., 2021). Previous studies have reported that the flux of DIC exceeds that of DOC in tidal ecosystems, although this finding is still debated (Call et al., 2019; Santos et al., 2019). DIC typically exhibits non-conservative behavior in estuary ecosystems, with its fate regulated by various factors (e.g., salinity and vegetation) (Tzortziou et al., 2011; Tan et al., 2020). The significant lateral enrichment of DIC in the low flat was likely to result from the case that the nearshore sites principally received more tidal seawater containing a greater amount of dissolved components per unit volume of the sediment column down to 10 cm, thereby elevating the DIC levels in the soil. On the other hand, it could also be attributable to the enhanced abiotic absorption of CO_2 induced by the lateral tidal flooding in the low flat, which is widely existed in inorganic carbon sequestration for high saline-alkali coastal soils (Wang et al., 2019). However, this needs further research to provide more direct evidence on the lateral tidal effect on the abiotic absorption of CO_2.

In addition to lateral outwelling, respiration was an important process for the export of fixed carbon in salt marshes. Although direct measurements of export gasses were not conducted in this study, soil microbial decomposition can be partially indicated by MBC and soil PLFAs. However, MBC exhibited no significant difference in tidal flats at different locations, while soil PLFAs tended to be abundant in the middle flat. This difference may be due to the different approaches used to measure microbial biomass. MBC was measured based on extracts and elements from lysed cells, representing the living part of soil organic matter (Kaur et al., 2005). On the other hand, PLFA is a constituent of living cell membranes (Kaur et al., 2005). Similar inconsistencies have been reported in previous studies (Leckie et al., 2004; Liu et al., 2018). Therefore, it is recommended to incorporate both indicators of microbial biomass for comprehensive results (Liu et al., 2018). Notably, PLFA analysis provides not only information on biomass but also taxonomic identity (Bossio and Scow, 1998). While most taxonomic PLFAs showed lateral enrichment in the middle flat, ProtozoaPLFA was found to be irresponsive to the lateral tidal effect, but varied along the vertical sedimentary gradient from land to sea. This also reflects divergent microbial inhabitation characteristics in response to the distinct vertical sedimentation and lateral tidal flooding in tidal flats.

5 Conclusions

This study demonstrates that the lateral tidal flooding through the tidal creeks in salt marsh exerts a marked effect on the distribution of carbon and nitrogen fractions. The divergent variation patterns of these carbon and nitrogen fractions ascross high, middle, and low flats demonstrate that the lateral tidal flooding has a strong impact on the sequestration of carbon in tidal salt marsh. Overall, the middle flat tended to be a hotpot of SOC, TN, and MBN variation, while DIC tended to be affected in the low flat under the influence of lateral tidal flooding. Significantly

lower relative variations of SOC in the middle flat induced by the lateral tidal effect may be ascribed to the enhanced microbial decomposition in the middle flat, suggested by concomitantly higher relative variations of microbial biomass as indicated by soil PLFAs and lower SOC levels. Additionally, better plant growth and denser creek distribution in the middle flat may also result in the reduction of SOC and TN levels due to increased nutrient uptake and superimposed scouring effects of multiple tidal creeks. However, the lateral enrichment of DIC in the low flat was possibly related to the greater amount of dissolved components contained in the seawater and/or abiotic adsorption, which needs further research. These findings underscore the critical role of lateral tidal effect in shaping the distribution patterns of carbon and nitrogen fractions in the soils of tidal salt marshes.

Data availability statement

The raw data supporting the conclusions of this article will be made available by the authors, without undue reservation.

Author contributions

ZM: Conceptualization, Writing – original draft, Writing – review & editing. YW: Data curation, Investigation, Writing – original draft. SZ: Formal analysis, Writing – original draft. YP: Visualization, Writing – original draft. JL: Methodology, Software, Writing – original draft. MZ: Funding acquisition, Supervision, Writing – review & editing. ZZ: Data curation, Supervision, Writing – review & editing.

Funding

Conflict of interest

The authors declare that the research was conducted in the absence of any commercial or financial relationships that could be construed as a potential conflict of interest.

Publisher's note

All claims expressed in this article are solely those of the authors and do not necessarily represent those of their affiliated organizations, or those of the publisher, the editors and the reviewers. Any product that may be evaluated in this article, or claim that may be made by its manufacturer, is not guaranteed or endorsed by the publisher.

Supplementary material

The Supplementary Material for this article can be found online at: https://www.frontiersin.org/articles/10.3389/fmars.2024.1361474/full#supplementary-material

References

Anderson, T. H., and Domsch, K. H. (1989). Ratios of microbial biomass carbon to total organic carbon in arable soils. *Soil Biol. Biochem.* 21, 471–479. doi: 10.1016/0038-0717(89)90117-X

Asanopoulos, C. H., Baldock, J. A., Macdonald, L. M., and Cavagnaro, T. R. (2021). Quantifying blue carbon and nitrogen stocks in surface soils of temperate coastal wetlands. *Soil Res.* 59, 619–629. doi: 10.1071/SR20040

Atwood, T. B., Connolly, R. M., Almahasheer, H., Carnell, P. E., Duarte, C. M., Ewers Lewis, C. J., et al. (2017). Global patterns in mangrove soil carbon stocks and losses. *Nat. Climate Change* 7, 523–528. doi: 10.1038/nclimate3326

Bossio, D. A., and Scow, K. M. (1998). Impacts of carbon and flooding on soil microbial communities: phospholipid fatty acid profiles and substrate utilization patterns. *Microbial. Ecol.* 35, 265–278. doi: 10.1007/s002489900082

Bossio, D. A., Scow, K. M., Gunapala, N., and Graham, K. J. (1998). Determinants of soil microbial communities: effects of agricultural management, season, and soil type on phospholipid fatty acid profiles. *Microbial. Ecol.* 36, 1–12. doi: 10.1007/s002489900087

Bouma, T. J., Friedrichs, M., Van Wesenbeeck, B. K., Temmerman, S., Graf, G., and Herman, P. M. J. (2009). Density-dependent linkage of scale-dependent feedbacks: A flume study on the intertidal macrophyte spartina anglica. *Oikos* 118 (2), 260–268.

Breithaupt, J. L., Smoak, J. M., Rivera-Monroy, V. H., Castañeda-Moya, E., Moyer, R. P., Simard, M., et al. (2017). Partitioning the relative contributions of organic matter and mineral sediment to accretion rates in carbonate platform mangrove soils. *Mar. Geology* 390, 170–180.

Call, M., Sanders, C. J., Macklin, P. A., Santos, I. R., and Maher, D. T. (2019). Carbon outwelling and emissions from two contrasting mangrove creeks during the monsoon storm season in palau, micronesia. *Estuarine Coast. Shelf Sci.* 218, 340–348.

Chang, D., Wang, Z., Ning, X., Li, Z., Zhang, L., and Liu, X. (2022). Vegetation changes in Yellow River Delta wetlands from 2018 to 2020 using PIE-Engine and short time series Sentinel-2 images. *Front. Mar. Sci.* 9, 977050. doi: 10.3389/fmars.2022.977050

Doran, J. W., Paul, E. A., and Clark, F. E. (2007). Soil microbiology and biochemistry. *J. Range Manage* 51 (2), 254. doi: 10.2307/4003217

Duarte, C. M., Losada, I. J., Hendriks, I. E., Mazarrasa, I., and Marbà, N. (2013). The role of coastal plant communities for climate change mitigation and adaptation. *Nat. Climate Change* 3, 961–968. doi: 10.1038/nclimate1970

England, P. R., Phillips, J., Waring, J. R., Symonds, G., and Babcock, R. (2008). Modelling wave-induced disturbance in highly biodiverse marine macroalgal communities: support for the intermediate disturbance hypothesis. *Mar. Freshw. Res.* 59, 515–520. doi: 10.1071/MF07224

Ensign, S. H., and Noe, G. B. (2018). Tidal extension and sea-level rise: recommendations for a research agenda. *Front. Ecol. Environ.* 16 (1), 37–43.

Fagherazzi, S., Wiberg, P. L., Temmerman, S., Struyf, E., Zhao, Y., and Raymond, P. A. (2013). Fluxes of water, sediments, and biogeochemical compounds in salt marshes. *Ecol. Processes* 2, 1–16. doi: 10.1186/2192-1709-2-3

Frostegård, A., and Bååth, E. (1996). The use of phospholipid fatty acid analysis to estimate bacterial and fungal biomass in soil. *Biol. Fertility soils* 22, 59–65. doi: 10.1007/BF00384433

Gabler, C. A., Osland, M. J., Grace, J. B., Stagg, C. L., Day, R. H., Hartley, S. B., et al. (2017). Macroclimatic change expected to transform coastal wetland ecosystems this century. *Nat. Climate Change* 7, 142–147. doi: 10.1038/nclimate3203

García-Orenes, F., Morugán-Coronado, A., Zornoza, R., and Scow, K. (2013). Changes in soil microbial community structure influenced by agricultural

management practices in a Mediterranean agro-ecosystem. *PloS One* 8, e80522. doi: 10.1371/journal.pone.0080522

Gerwing, T. G., Gerwing, A. M. A., Macdonald, T., Cox, K., Juanes, F., and Dudas, S. E. (2017). Intertidal soft-sediment community does not respond to disturbance as postulated by the intermediate disturbance hypothesis. *J. Sea Res.* 129, 22–28. doi: 10.1016/j.seares.2017.09.001

Glaser, C., Frei, S., Massmann, G., and Gilfedder, B. S. (2021). Tidal creeks as hot-spots for hydrological exchange in a coastal landscape. *J. Hydrol.* 597, 126158. doi: 10.1016/j.jhydrol.2021.126158

Han, X., Gao, G., Chang, R., Li, Z., Ma, Y., Wang, S., et al. (2018). Changes in soil organic and inorganic carbon stocks in deep profiles following cropland abandonment along a precipitation gradient across the Loess Plateau of China. *Agric. Ecosyst. Environ.* 258, 1–13. doi: 10.1016/j.agee.2018.02.006

Kaur, A., Chaudhary, A., Kaur, A., Choudhary, R., and Kaushik, R. (2005). Phospholipid fatty acid–a bioindicator of environment monitoring and assessment in soil ecosystem. *Curr. Sci.* 89 (7), 1103–1112.

Kelleway, J. J., Saintilan, N., Macreadie, P. I., Baldock, J. A., Heijnis, H., Zawadzki, A., et al. (2017). Geochemical analyses reveal the importance of environmental history for blue carbon sequestration. *J. Geophysical Research: Biogeosciences* 122, 1789–1805. doi: 10.1002/2017JG003775

Knobloch, A. L., Reay, W. G., and Canuel, E. A. (2021). Carbon pools differ in source and temporal patterns in a tidal marsh creek system of the York River, VA Estuary. *Estuaries Coasts* 44, 1848–1865. doi: 10.1007/s12237-020-00878-y

Krest, J. M., Moore, W. S., Gardner, L. R., and Morris, J. T. (2000). Marsh nutrient export supplied by groundwater discharge: Evidence from radium measurements. *Global Biogeochemical Cycles* 14, 167–176. doi: 10.1029/1999GB001197

Lai, S., Yaakub, S. M., Poh, T. S., Bouma, T. J., and Todd, P. A. (2018). Unlikely nomads: settlement, establishment, and dislodgement processes of vegetative seagrass fragments. *Front. Plant Sci.* 9, 328860.

Lal, R. (2008). Carbon sequestration. *Philos. Trans. R. Soc. B: Biol. Sci.* 363, 815–830. doi: 10.1098/rstb.2007.2185

Lavelle, J. W., Massoth, G. J., and Crecelius, E. A. (1985). *Sedimentation rates in Puget Sound from ^{210}PB measurements. NOAA Technical Memorandum ERL PMEL-61*. Seattle, Washington: Contribution (Pacific Marine Environmental Laboratory (U.S.)), 732. https://repository.library.noaa.gov/view/noaa/9479.

Leckie, S. E., Prescott, C. E., Grayston, S. J., Neufeld, J. D., and Mohn, W. W. (2004). Comparison of chloroform fumigation-extraction, phospholipid fatty acid, and DNA methods to determine microbial biomass in forest humus. *Soil Biol. Biochem.* 36, 529–532. doi: 10.1016/j.soilbio.2003.10.014

Liu, D., Huang, Y., Sun, H., and An, S. (2018). The restoration age of Robinia pseudoacacia plantation impacts soil microbial biomass and microbial community structure in the Loess Plateau. *Catena* 165, 192–200. doi: 10.1016/j.catena.2018.02.001

Ma, Z., Wu, Y., Cui, Y., Pan, Y., Zhao, S., Liu, J., et al. (2024). Coastal distribution and driving factors for blue carbon fractions in the surface soil of a warm-temperate salt marsh in China. *Chemosphere* 350, 141044. doi: 10.1016/j.chemosphere.2023.141044

Ma, Z., Zhang, M., Xiao, R., Cui, Y., and Yu, F. (2017). Changes in soil microbial biomass and community composition in coastal wetlands affected by restoration projects in a Chinese delta. *Geoderma* 289, 124–134. doi: 10.1016/j.geoderma.2016.11.037

Mcleod, E., Chmura, G. L., Bouillon, S., Salm, R., Björk, M., Duarte, C. M., et al. (2011). A blueprint for blue carbon: toward an improved understanding of the role of vegetated coastal habitats in sequestering CO2. *Front. Ecol. Environ.* 9, 552–560. doi: 10.1890/110004

Nguyen, H. Y. T., Cao, D. M., and Schmitt, K. (2013). Soil particle-size composition and coastal erosion and accretion study in Soc Trang mangrove forests. *J. Coast. Conserv.* 17, 93–104. doi: 10.1007/s11852-012-0221-4

Ning, Z., Li, D., Chen, C., Xie, C., Chen, G., Xie, T., et al. (2023). The importance of structural and functional characteristics of tidal channels to smooth cordgrass invasion in the Yellow River Delta, China: Implications for coastal wetland management. *J. Environ. Manage.* 342, 118297. doi: 10.1016/j.jenvman.2023.118297

Odum, E. P. (1963). *Ecology*. Modern Biology Series. Eds. H. Rinehart and W. New York (New York (NY, USA): Holt, Rinehart and Winston).

Odum, E. (2002). "Tidal Marshes as Outwelling/Pulsing Systems," in *Concepts and Controversies in Tidal Marsh Ecology* (Kluwer Academic Publishers, New York), 3–7.

Olsson, P. A. (1999). Signature fatty acids provide tools for determination of the distribution and interactions of mycorrhizal fungi in soil. *FEMS Microbiol. Ecol.* 29, 303–310. doi: 10.1111/fem.1999.29.issue-4

Olsson, P. A., Bååth, E., Jakobsen, I., and Söderström, B. (1995). The use of phospholipid and neutral lipid fatty acids to estimate biomass of arbuscular mycorrhizal fungi in soil. *Mycological Res.* 99 (5), 623–629.

Pedersen, M.Ø., Serrano, O., Mateo, M. A., and Holmer, M. (2011). Decomposition of Posidonia oceanica matte in a climate change setting. *Aquat. Microb. Ecol.* 65, 169–182. doi: 10.3354/ame01543

Peng, G., Xiang, N., Lv, S. Q., and Zhang, G. C. (2014). Fractal characterization of soil particle-size distribution under different land-use patterns in the Yellow River Delta Wetland in China. *J. Soils Sediments* 14, 1116–1122. doi: 10.1007/s11368-014-0876-6

R Core Team (2021). *R: A language and environment for statistical computing* (Vienna, Austria: R Foundation for Statistical Computing). Available at: http://www.R-project.org/.

Rabot, E., Wiesmeier, M., Schlüter, S., and Vogel, H. J. (2018). Soil structure as an indicator of soil functions: A review. *Geoderma* 314, 122–137.

Regier, P., Ward, N. D., Indivero, J., Wiese Moore, C., Norwood, M., and Myers-Pigg, A. (2021). Biogeochemical control points of connectivity between a tidal creek and its floodplain. *Limnol. Oceanogr. Lett.* 6, 134–142. doi: 10.1002/lol2.10183

Ren, J., Chen, J., Xu, C., van de Koppel, J., Thomsen, M. S., Qiu, S., et al. (2021). An invasive species erodes the performance of coastal wetland protected areas. *Sci. Adv.* 7, eabi8943. doi: 10.1126/sciadv.abi8943

Sanders, C. J., Maher, D. T., Tait, D. R., Williams, D., Holloway, C., Sippo, J. Z., et al. (2016). Are global mangrove carbon stocks driven by rainfall? *J. Geophysical Research: Biogeosciences* 121, 2600–2609. doi: 10.1002/2016JG003510

Santini, N. S., Lovelock, C. E., Hua, Q., Zawadzki, A., Mazumder, D., Mercer, T. R., et al. (2019). Natural and regenerated saltmarshes exhibit similar soil and belowground organic carbon stocks, root production and soil respiration. *Ecosystems* 22, 1803–1822. doi: 10.1007/s10021-019-00373-x

Santos, I. R., Burdige, D. J., Jennerjahn, T. C., Bouillon, S., Cabral, A., Serrano, O., et al. (2021). The renaissance of Odum's outwelling hypothesis in'Blue Carbon'science. *Estuarine Coast. Shelf Sci.* 255, 107361. doi: 10.1016/j.ecss.2021.107361

Santos, I. R., Maher, D. T., Larkin, R., Webb, J. R., and Sanders, C. J. (2019). Carbon outwelling and outgassing vs. burial in an estuarine tidal creek surrounded by mangrove and saltmarsh wetlands. *Limnol. Oceanogr.* 64, 996–1013. doi: 10.1002/lno.11090

Studds, C. E., Kendall, B. E., Murray, N. J., Wilson, H. B., Rogers, D. I., Clemens, R. S., et al. (2017). Rapid population decline in migratory shorebirds relying on Yellow Sea tidal mudflats as stopover sites. *Nat. Commun.* 8, 14895. doi: 10.1038/ncomms14895

Tan, L., Ge, Z., Fei, B., Xie, L., Li, Y., Li, S., et al. (2020). The roles of vegetation, tide and sediment in the variability of carbon in the salt marsh dominated tidal creeks. *Estuarine Coast. Shelf Sci.* 239, 106752. doi: 10.1016/j.ecss.2020.106752

Taniguchi, M., Dulai, H., Burnett, K. M., Santos, I. R., Sugimoto, R., Stieglitz, T., et al. (2019). Submarine groundwater discharge: updates on its measurement techniques, geophysical drivers, magnitudes, and effects. *Front. Environ. Sci.* 7, 141.

Tzortziou, M., Neale, P. J., Megonigal, J. P., Pow, C. L., and Butterworth, M. (2011). Spatial gradients in dissolved carbon due to tidal marsh outwelling into a Chesapeake Bay estuary. *Mar. Ecol. Prog. Ser.* 426, 41–56. doi: 10.3354/meps09017

van Ardenne, L. B., Jolicouer, S., Bérubé, D., Burdick, D., and Chmura, G. L. (2018). The importance of geomorphic context for estimating the carbon stock of salt marshes. *Geoderma* 330, 264–275. doi: 10.1016/j.geoderma.2018.06.003

Vance, E. D., Brookes, P. C., and Jenkinson, D. S. (1987). An extraction method for measuring soil microbial biomass C. *Soil Biol. Biochem.* 19, 703–707. doi: 10.1016/0038-0717(87)90052-6

Wang, X., Jiang, Z., Li, Y., Kong, F., and Xi, M. (2019). Inorganic carbon sequestration and its mechanism of coastal saline-alkali wetlands in Jiaozhou Bay, China. *Geoderma* 351, 221–234. doi: 10.1016/j.geoderma.2019.05.027

Wang, Q., Xie, T., Luo, M., Bai, J., Chen, C., Ning, Z., et al. (2021). How hydrological connectivity regulates the plant recovery process in salt marshes. *J. Appl. Ecol.* 58, 1314–1324. doi: 10.1111/1365-2664.13879

Webb, J. R., Santos, I. R., Maher, D. T., Tait, D. R., Cyronak, T., Sadat-Noori, M., et al. (2019). Groundwater as a source of dissolved organic matter to coastal waters: Insights from radon and CDOM observations in 12 shallow coastal systems. *Limnol. Oceanogr.* 64, 182–196. doi: 10.1002/lno.11028

Windham-Myers, L., Cai, W.-J., Alin, S. R., Andersson, A., Crosswell, J., Dunton, K. H., et al. (2018). "Chapter 15: Tidal wetlands and estuaries," in *Second state of the carbon cycle report (SOCCR2): a sustained assessment report*. Eds. N. Cavallaro, G. Shrestha, R. Birdsey, M. A. Mayes, R. G. Najjar, S. C. Reed, P. Romero-Lankao and Z. Zhu (U.S. Global Change Research Program, Washington), 596–648. doi: 10.7930/SOCCR2.2018.Ch15

Wu, Y., Liu, J., Yan, G., Zhai, J., Cong, L., Dai, L., et al. (2020). The size and distribution of tidal creeks affects salt marsh restoration. *J. Environ. Manage.* 259, 110070. doi: 10.1016/j.jenvman.2020.110070

Wu, Y., Zhang, Z., Hipsey, M., and Zhang, M. (2023a). Tides as a key factor driving effective seed dispersal in coastal wetlands. *Ecol. Indic.* 148, 110110. doi: 10.1016/j.ecolind.2023.110110

Wu, Y., Zhang, Z., Hipsey, M. R., and Zhang, M. (2023b). Tidal action enhances coastal wetland plant connectivity. *Chemosphere* 331, 138784. doi: 10.1016/j.chemosphere.2023.138784

Wu, Y., Zhao, S., Dai, L., Liu, Y., Xie, L., Zhang, Z., et al. (2021). Tides affect plant connectivity in coastal wetlands on a small-patch scale. *Chemosphere* 262, 127977. doi: 10.1016/j.chemosphere.2020.127977

Zelles, L., Bai, Q. Y., Rackwitz, R., Chadwick, D., and Beese, F. (1995). Determination of phospholipid-and lipopolysaccharide-derived fatty acids as an estimate of microbial biomass and community structures in soils. *Biol. Fertility Soils* 19, 115–123.